Bandaru Kiran

B.Tech, School of Mechanical Engineering (SMEC)
Vellore Institute of Technology (VIT)
Vellore, Tamil Nadu
India

Kaushik Mishra

B.Tech, School of Mechanical Engineering (SMEC)
Vellore Institute of Technology (VIT)
Vellore, Tamil Nadu
India

Yash Raj Singh

B.Tech, School of Mechanical Engineering (SMEC)
Vellore Institute of Technology (VIT)
Vellore, Tamil Nadu
India

Dega Nagaraju

Professor
Department of Manufacturing Engineering
School of Mechanical Engineering (SMEC)
Vellore Institute of Technology (VIT)
Vellore, Tamil Nadu
India

Structural and Thermal Analysis of Butt Joint GTAW of Similar and Dissimilar Materials with Distinct Groove Angles Through Simulation and Mathematical Modelling

The present article discusses the simulation and mathematical modelling of GTAW for various parameters of single and double V-groove butt joint welds. The chosen materials are EN 10025steel(grade S295) and D36 ship building steel, owing to their wide industrial applications and corrosion resistive nature. The simulation modelling was carried out at 90°, 60°, 45° and 30° groove angles for both similar and dissimilar base metals to predict the deformation, residual stress distribution, heat flux, and nodal temperature using ABAQUS software package. A subsequent mathematical model was developed using MATLAB tool to further predict the temperature distribution and total stress concentration at any localized nodal point. The model can be used to obtain optimal weld parameters such as weld, speed torch temperature, current and voltage. The obtained results were plotted to attain the clear conclusion over the results. The results under simulation showed 45° to be the most effective angle for both Single-V and Double-V grooved butt joints.

Keywords: *GTAW; Single and Double V-groove; Simulation and Mathematical modelling; Butt joint; ABAQUS; MATLAB; EN 10025 Steel; Ship Building Steel.*

1. INTRODUCTION

Welding is predominantly used in all the mechanical applications for the development of mechanical joints because of its strength, flexibility and low cost. Welding is treated as a complex manufacturing process that results in high residual stresses, irregular dimensions and metal imperfections. High tensile residual stresses generated in welding have a high impact on fatigue life of components and hence it is a high concern in design of the product. The residual stresses, deformation and temperature modelling is a complex task which use the welding parameters at high temperatures.Low carbon steels are less susceptible to corrosion than steels richer in carbon.It has a large scope of utilization in the regions of waste treatment, vent-gas desulfurization systems and vastly in non-destructive impact testing in any condition.EN 10025 steel has a relatively high resistance to breakage. Mild steel has a carbon composition and it is malleable, even in cold conditions. It means it has high tensile strength and correspondingly higher impact strength. Mild steel bends or deforms but does not crack or shatter. Welding is a fabrication or sculptural process for joining metals, usually metals or thermoplastics. It is done by applying high amount of heat, which results in dissolving of metal at the joint

between two sections making it intermix for the most part, with a transitional liquid filler material [1]. A metallic bond is made when it is cooled and solidified. The last weldment has comparable quality properties as the metal which is difficult to get in non-fusion forms [1, 3]. It is because of the intermixing of metals during the welding. A filler material is used to add it in the joint to frame a pool of liquid material (the weld pool) that cools to shape a joint. Weld parameters (butt joint, depth of penetration, type of fillet and so on) choose the quality of the joint which can be stronger than the base metal or parent material [2]. In any case, there are different perspectives which have sway on the quality and properties of the weldment [1, 4]. For example, a distribution of high amount of residual stresses over the span of welding can cause distortion in cases [1, 4]. Arc welding is an effective and economical joining process to produce welded joints of high strength. During any arc welding process, due to different types of heating and cooling rates non-uniform expansion and contraction of the weld occurs which results in residual stresses (RS) in weld area [5]. These RS are unsuitable for the service life and structural integrity of weld areas. The RS can be tensile and compressive which will affect strength of the welded joints. Fatigue failure and brittle fracture occurs due to the tensile RS and yield properties of welded joints can be increased by compressive RS [6]. The nature of Residual stresses mostly depends on heat input, number of passes, dimensions of base plate, welding speed, type of joint and type of clamping used [7]. In Gas Tungsten Arc Welding (GTAW) Heat Affected Zone (HAZ) will be higher due

to enlargement of width of weld pool because of continuous heat inputs [8]. These heat inputs can be varied by changing pulse frequency modes which will further decrease the HAZ, thermal stresses and total deformations [9]. By varying the thickness of the base metal RS can be minimised i.e. less RS in thicker plates [10]. The welding speed and current affects the heat distribution at HAZ [11]. Clamping base metal during welding affects theweld specimen. Longitudinal stresses can be observed more in clamped specimens than inunclamped ones because clamping doesn't allow base metal to distort hence RS develop [12]. V-groove base metal reduces longitudinal stresses morethan U-groove type [13]. Tensile residual stresses are inversely proportional to the welding length and welding speed. RS are minimum in symmetric welding of carbon steel samples [14]. Post heat treatment process (tempering) relieves RS developed in weld area [15]. Hence, to develop highly efficient welded structures prediction of nodal temperature and RS is helpful. Finite element analysis (FEA) is most commonly used for analysing structural (RS and deformation) and thermal (nodal temperature and heat flux) results of weldments. The distortions developing in the weld area are not only because of shrinkage due to cooling but also due to disarrangement of base plates to be welded and root gap [16]. The austeniticheat treated steels are corrosion and oxidation safe because of the presence of chromium that frames a self-mending defensive film on the surface of the steel. They likewise have great sturdiness at incredibly low temperatures hence are utilized widely in cryogenic applications. They can be hardened and their strength can be increased by cold working but not by heat treatment. The separate metals joining of tempered steel and copper have a few applications in nuclear industry, chemical and automotive divisions. The welding procedure presents difficulties because of the complex weld pool improvement inferable from the distinction in material properties as dissolving point, thermal conductivity and others.

2. LITERATURE REVIEW

Dhas and Kumanan [17] investigated HAZ characteristics, and also essential weld size and bead quality. Moarrefzadeh and Branch [18] analysed the effects of current characteristics. Anca et al. [19] disclosed that to improve efficiency and nature of weld, understanding the impact of various parameters is a key to answering the issue. Mahapatra et al. [20] did investigation on impact process parameters on temperature dispersions and anticipated various zones of miniaturized scale structure for butt joint and fillet weld joint. According to M.S. Starvin et al. [21] FEA utilizing Norton's creep law is completed at high temperature to anticipate the creep of the welded joint. Acevedo et al. [4] applied numerical techniques for understanding the initial stress concentrations. Dascau et al [22] have explored on the plunge stage in FSW utilizing mathematical analysis, did classification of heat generation during the procedure and also performed analysis of the plunge stage utilizing two distinct tools in the numerical analysis. According to Masubuchi et al [26], the heat generated in

friction stir welding can be isolated into three sections: frictional heat produced by the tool shoulder, frictional heat created by the tool pin, and heat produced by material plastic distortion close to the pin area. The main disadvantages during weldingare the presence of distortions and residual stresses developed in the work piece which will affect the work piece life. The movement of the molten weld causes thermal gradients in the material which induces residual stresses and deformation in the work piece iswell addressed [27, 28]. Approximate calculations have been carried out to measure residual stresses as is done in [13]. The research work in the field of TIG welding and different simulation sequences educated by Ding-fa Fu [2] provide the important aspect of stresses. The study of temperature history of P92 Steel by A.H. Yaghi et al [23] after arc welding of dissimilar materials provides aprediction technique. The major outcome from this work is the process of applying finite element method in Abaqus to numerically simulate welding residual stresses.Unlike all the above mentioned articles, in this paper, work is carried out in evaluating residual stress and deformation of mild steel in case of tungsten inert gas welding utilizing ABAQUS software for simulation. By considering the Indian Welding Journal distributed by Indian Welding Society, it is seen that distortion and residual stresses increase withan increment of the groove angle. Joint quality additionally increases with groove angle increment of the welded material which influences the economy of welding. Incompanies facing issues related with weld quality, the V-groove geometry can utilize better outcomes acquired from this investigation. Selection of a specific kind of groove geometry is affected by two primary factors: a) machining cost to get wanted groove geometry,and b) cost of weld material (based on volume), unlike different factors such as welding speed, availability of groove angle, residual stresses and distortion control necessity.

In this development, the most productive V-groove angle is chosen depending on the results of residual stresses, distortions, nodal temperature, and heat-flux considering similar and dissimilar metals welding. Opposite to V and bevel groove, geometries can effectively and financially be created by machining or gas cutting other than heating up to the base of the section. V-groove butt welds are for the most part utilized for basic applications where tension and fatigue is normal during the process. Since butt groove geometry doesn't cause any pressure restriction, stresses created in welded joints, because of external stacking to a great extent, become uniform over the segment of the weld. Henceforth, fatigue crack nucleation is fundamentally brought down in butt groove welds in contrast to fillet and other welds.

3. FEA SOFTWARE - ABAQUS

ABAQUS/Complete ABAQUS Environment is a mechanical software utilized to design and simulate any mechanical part, assembly and envisions their FEM result [24]. ABAQUS/CAE likewise gives a particular module to perform welding simulations called ABAQUS Welding Interface (AWI) [25]. AWI is the interface which

first leads a transient thermal analysis and makes another model for structural simulation of the welded part. It uses the yield of transient thermal analysis and accepts the temperature variations as a contribution to structural simulation. It requires different sources of inputs, such as material properties, the melting point, Boltzmann's constant, meshing details, etc. Every FEM model comprises of three phases. Modelling and pre-processing is the initial phase where an input model is made which consists of material properties, part model, meshing, load and boundary conditions of the model. In thethird stage, post-processing, results are seen as animations of various loads or temperatures whichever appropriate. The prerequisites of AWI to perform welding analysis are material properties at variable temperature, weld plate and weld measurements, weld temperature, ambient temperature, Boltzmann constant and interaction properties between the material.

4. METHODOLOGY

Detailed explanation of the Abaqus simulation, i.e. thermal and structural simulation is mentioned in the figure 5 below. In the initial step, a weld plate of explicit measurements is produced and weld beads are made by isolating the weld area into a required number of segments utilizing the partition tool. Schematic representation of single and double V groove angles are shown in figure 1 and 2 below.
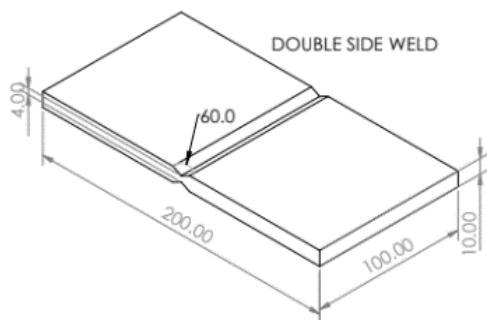
Figure 1. Schematic representation of single V groove design.
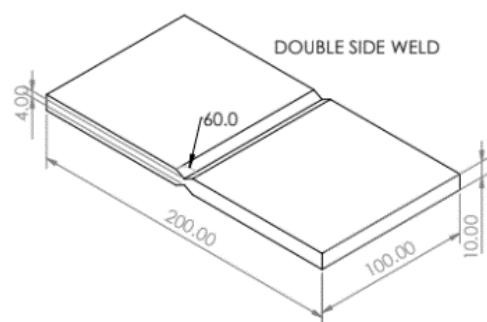
Figure 2. Schematic representation of double V groove design.

Required material properties are -(i) density for mild steel (7850kg/m³), (ii) modulus of elasticity , (iii) heat transfer coefficient, (iv) Poisson's ratio, (v) coefficient of thermal expansion for shipbuilding steel is $12 \cdot 10^{-6}$ °C^{-1}, (vi) yield stress, (vii) plastic strain, (viii) specific heat, (ix) thermal conductivity, (x) temperature, (xi) enthalpy.

All the properties should be in S.I units. After defining the material properties, a solid homogeneous section is defined and assigned to the weld plate, as the weld plate and weld material are the same, these both can be assigned the same section.

The model is meshed prior to inputting the AWI. At this stage meshing need not be perfect as it can be modified in the AWI, but it is necessary because without meshing the model, we cannot start AWI. In Figure 2 the applied meshing is, DC3D4, i.e. a 4-node linear heat transfer tetrahedron.
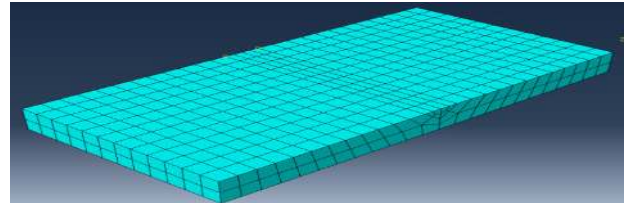

Figure 2. Meshed model

For performing welding in AWI, the base metal must be drawn using ABAQUS programming or it can be built using CAD software like Solidworks or Catia and be imported into ABAQUS. After the weld plate is made, weld temperature (1600°C), ambient temperature (25°C), melting point of metal (1580°C), Stefan-Boltzmann constant and absolute zero temperature (-273°C) need to be characterized. In AWI, weld beads have to be defined. Once all the beads are selected then pass controls are defined which means temperature can be controlled during applying and lifting of the weld torch. After this step, the weldpasses are defined. This procedure is carried out for similar metals (plain carbon steel) and dissimilar metals (plain carbon steel and D36 shipbuilding steel) by considering the below properties shown in Tables 1, 2, and 3.

Table 1. No of passes in each groove

Groove angles	No. of passes	
	Single V	Double V
90	2	2
60	2	2
45	1	2
30	1	1

Making employments from AWI will overwrite any past settings made in the ABAQUS Modeler. It makes two distinct models first for thermal examination and the second for structural. First the thermal model is run because its results will be used for the structural model. Before running the structural model constraint, the model at the sides should be fixed and after fixing the model, the model is run and results can be analysed.
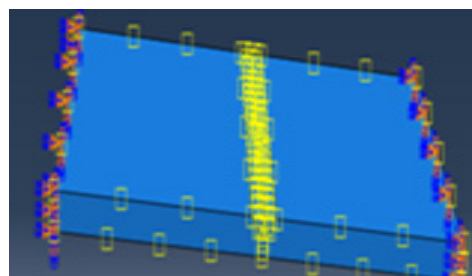

Figure 3. Base plate with Boundary conditions

Table 2. Mechanical and Thermal properties of EN 10025 Steel plate

Temperature (°C)	Thermal Conductivity (W/m°C)	Specific Heat (J/kg°C)	Young's Modulus (GPa)	Thermal Coefficient (10^{-5} °C^{-1})	Enthalpy (10^9 J/m^3)	Poisson's Ratio	Yield Stress (MPa)
0	51.9	450	200	1.00	1	0.2786	290
100	51.1	499.2	200	1.10	2	0.3095	260
300	46.1	565.5	200	1.20	2.65	0.331	200
450	41.05	630.5	150	1.30	3.8	0.338	150
550	37.5	705.5	110	1.40	4.1	0.3575	120
600	35.6	773.3	88	1.40	4.55	0.3738	110
720	30.64	1080.4	20	1.40	5	0.3738	9.8
800	26	931	20	1.40	5.23	0.4238	9.8
1450	29.45	437.93	2	1.50	9	0.4738	0.2
1510	29.7	400	0.2	1.50	11	0.494	0.1
1580	29.7	735.25	2×10^{-5}	1.50	11	0.494	0.0098
5000	42.2	400	2×10^{-5}	1.55	12.5	0.494	0.0098

Table 3. Mechanical and Thermal properties of D36 Shipbuilding steel plate

Temperature (°C)	Thermal Conductivity (W/m°C)	Specific Heat (J/kg°C)	Density (Kg/m^3)	Young's Modulus (GPa)	Poisson's Ratio	Yield Stress (MPa)	Tangential Modulus (GPa)
20	35.1	427	7860	199.67	0.3	371.9	10.78
200	36.8	502	7795	199.3	0.32	362.1	10.71
300	36.8	548	7759	198.04	0.331	347	10.58
400	36.2	602	7725	192.9	0.34	317.5	10.1
500	34.6	665	7690	174	0.353	267.9	18.87
600	32.0	741	7654	125.3	0.364	202.8	6.52
700	28.5	1481	7620	61.7	0.375	139.8	3.72
760	25.8	686	7609	45.3	0.39	100	1.8
900	26.6	653	7604	14.9	0.397	69.2	0.94
1000	27.2	653	7604	12.02	0.4	56.3	0.622
1100	27.8	653	7604	11.32	0.419	50.35	0.514
1200	28.4	653	7604	11.1	0.43	47.65	0.479
1300	29.0	653	7604	11.1	0.441	46.4	0.467
1400	29.6	653	7604	11.1	0.452	45.9	0.463

Points and standards of boundary conditions are defined in the methodology to obtain results. Both ends are fixed, arresting all degrees of freedom. Workpiece under clamping condition is represented in the figure 3 above.

5. MATHEMATICAL MODELLING

The design strength of a weldment is controlled by either the strength of the weld metal or the base metal.

$$S_w = \frac{F_w}{A_w} \tag{1}$$

$$S_{BM} = \frac{F_{BM}}{A_{BM}} \tag{2}$$

(1) depicts the strength of weld metal and (2) depicts the strength at the base metal.

Similar to a Complete-Joint-Penetration weld type, the effective cross-sectional area of a Partial-Joint-Penetration groove weld is equal to the effective throat times the length of the weld which is mathematically expressed as given in (3). However, the effective throat thickness of the partial penetration weld is less than either of the plate thicknesses being joined.

$$A_w = t_e L_w \tag{3}$$

For design purposes, it is often convenient to express the design strength of a fillet weld per inch of length rather than the design weldment strength.

$$K_w = \frac{S_w}{t_e} \tag{4}$$

For a given factored design load, the required weld length can be determined as a ratio of the parameterized design load and design strength per inch of the weld segment:

$$L_{req} = \frac{P_n}{K_w} \tag{5}$$

The design of a groove joint is relatively simple since effective area at the weld, A_w is equal to the projection of the groove at the workpiece area. For groove type welds subject to tension (as in butt splice), the strength of the weld zone has to match that of the workpiece. No explicit design of the weld is required. If plates of different areas are joined, the design strength of the plate is governed by the plate having the smaller cross-sectional area. The groove angle and the weld depth are calculated as given in Figure 4.

Fig.4. Weld groove geometry specification

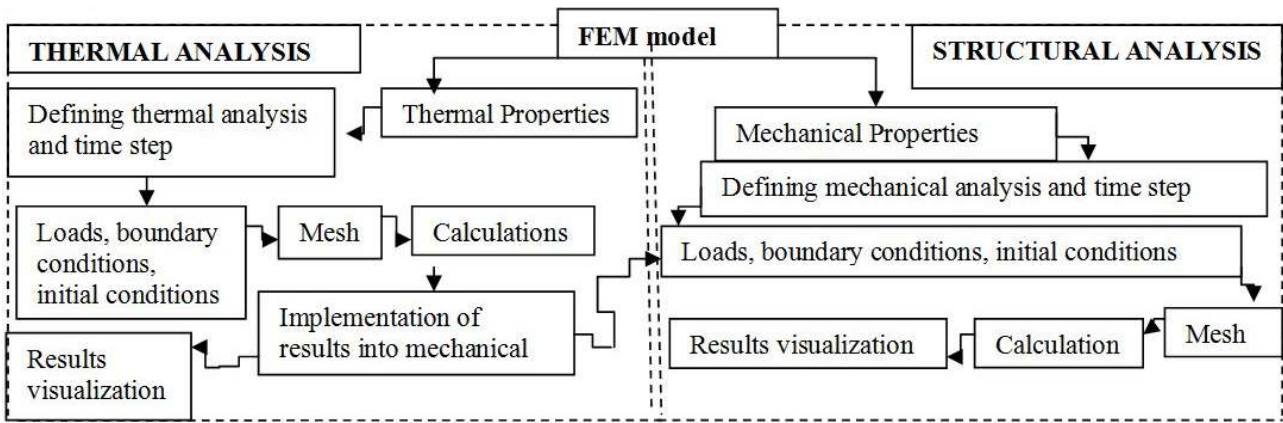Condition for P-J-P weld: If $45° < \alpha < 60°$; then the throat thickness is $t_e = D - \frac{1}{8}$ inches.

Figure 5. Flow chart of simulation modelling in ABAQUS

Condition for C-J-P weld : If $\alpha \geq 60°$; $t_e = D$ inches.

Partial-Joint-Penetration groove welds subject to tension normal to the effective cross-sectional area must be designed for both weld metal and base material.

The weld metal and base metal strength as per Table J2.5 of AISC specification is given in (6) and (7) respectively.

$$S_w = 0.80 \times 0.60 \times \frac{F_{EX}}{A_w} \qquad (6)$$

$$\phi S_{BM} = 0.9 \times \frac{F_y}{A_{BM}} \qquad (7)$$

It assumes to be the area of the plate adjacent to the weld yields. When a P-J-P groove weld is subjected to compression load which is normal to the weld zone or either tension or compression parallel to the axis of the weld zone, only the strength of the base material has to be checked.

For partial penetration in groove welds which are subject to shear, both weld metal and base metal strength must be checked as per Table J2.5 of AISC specification given in (8a) and (8b) respectively.

$$\phi \frac{F_w}{A_w} = 0.75 \times 0.60 \times \frac{F_{EX}}{A_w} \qquad (8a)$$

$$\phi P_n = 0.75 \times \frac{F_y}{A_{nv}} \qquad (8b)$$

The factored design strength per inch can also be expressed as a function of gross cross-sectional area of the plate which is subjected to shear loading as given in (9):

$$\phi P_n = 0.9 \times 0.60 \times \frac{F_y}{A_{gt}} \qquad (9)$$

The results obtained from the simulation model, the values of stress concentration, temperature distribution and residual stress are employed in the mathematical equations. The stress results are formulated in a stress matrix using R program. The matrix is developed using regression correlation statistical method as shown in (10). The temperature distribution coefficients are calculated using linear regression analysis which is also done using R software. The obtained coefficient values are plugged in a two-dimensional

regression equation using MATLAB. Cubic spline curve fitting method is used to form a generalized mathematical model using the obtained correlation constants of both stress matrix and temperature distribution equation. A SIMULINK model is also developed to validate the model.

A precise mathematical model properly justifies the abstract of carried work and falls within an error window of 8-13% with respect to the simulated model.

$$Y = b_0 + \sum_{i=1}^{i=n} b_i x_i + \sum_{i=1}^{i=n-1} \sum_{j=i+1}^{j=n} b_{ij} x_i y_j + \sum_{i=1}^{i=n} b_i x_i^2 \qquad (10)$$

By equating the quantity of heat energy during influx and outflux at the instant of welding and considering heat loss to be only by conduction, the temperature at any instant is given by (11).
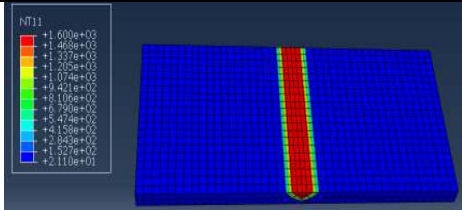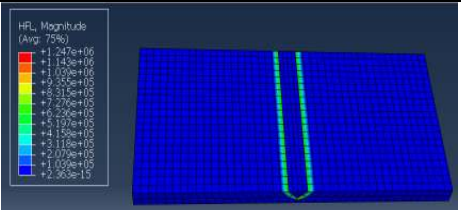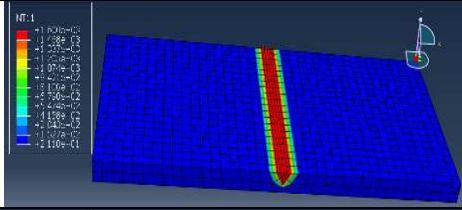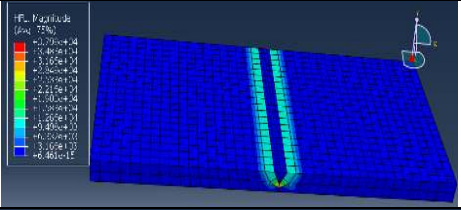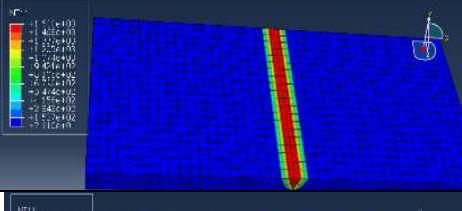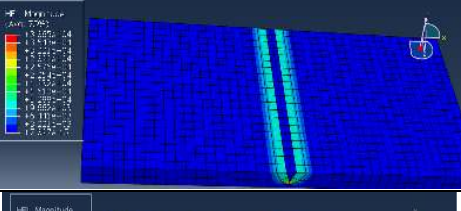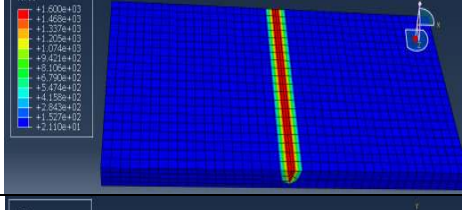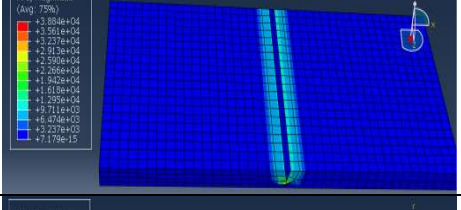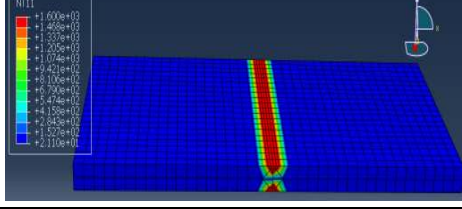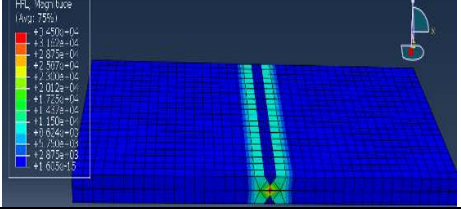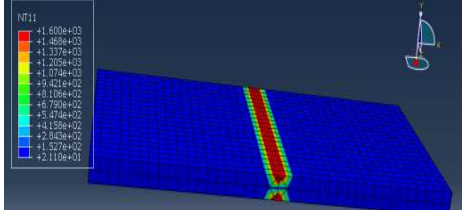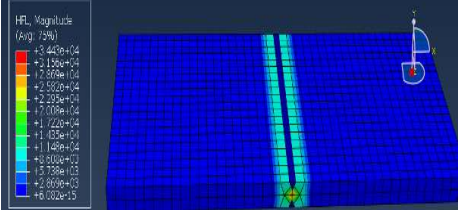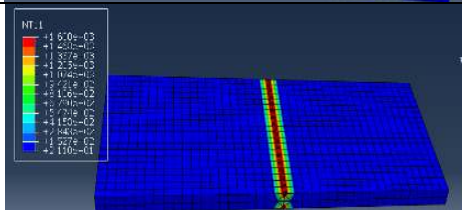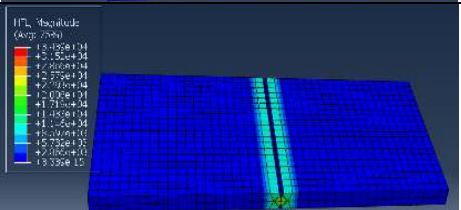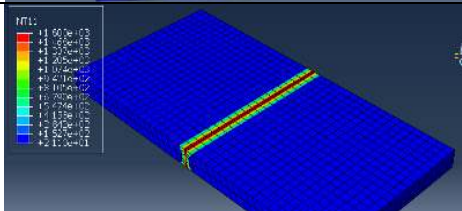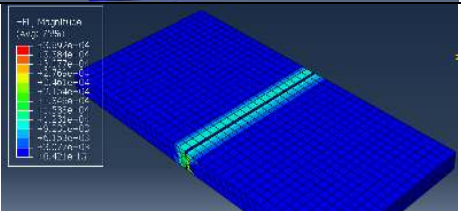
$$T - T_0 = \frac{Q}{2\pi k R} e^{-\lambda v + (x - vt)\lambda} \qquad (11)$$

6. RESULTS AND DISCUSSIONS

6.1 Thermal analysis of nodal temperature

The temperature distribution in fusion zone and heat affected zone for similar welded butt joints are mapped to its transverse and longitudinal node points and are illustrated in tables 4 and 6. The simulation results of temperature distributions around heat affected zone (HAZ) and fusion zone (FZ) are shown in above Tables. It is also identified in simulation that small area of weld plate gets preheated by moving heat source. The maximum temperature (1600°C exactly equal to torch temperature) can be seen in the fusion zone (FZ) and is proportional to the given heat input. The heat generated by the moving torch gradually descends and is transferred to the base plate by conduction, convection (natural convection) and radiation. The maximum temperature is 1600°C that equals the input torch temperature, whereas, the minimum temperature is 25°C i.e. the designated ambient temperature. The observations conclude thathigh temperature distributionis noticed in larger V-groove angles, because of larger V-groove volume. Hence, grains formed are finer and the material ultimately produced is harder.

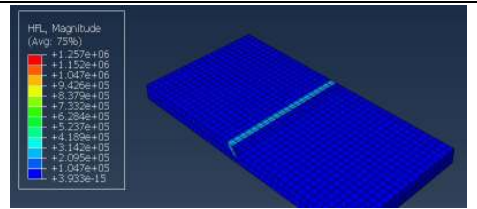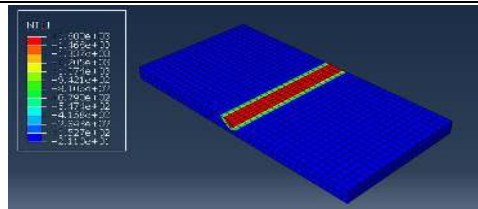**Table 4. Thermal analysis results for similar and dissimilar materials welding**

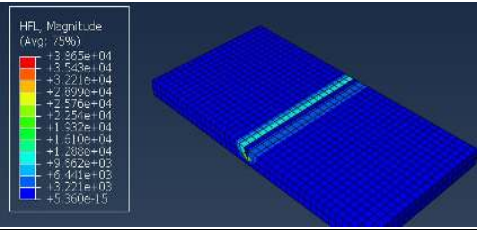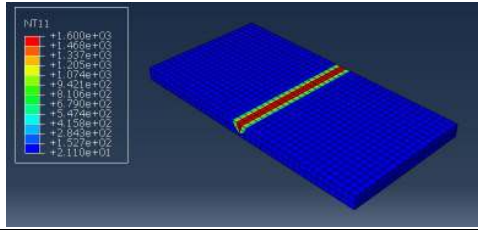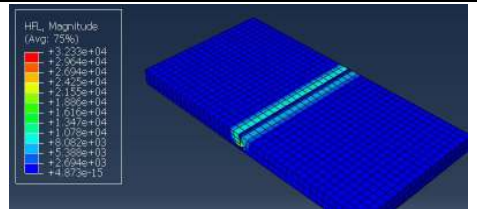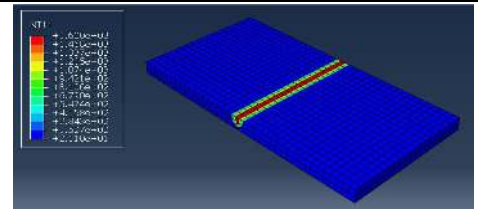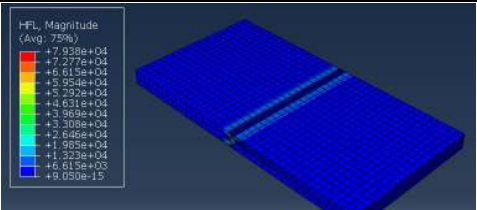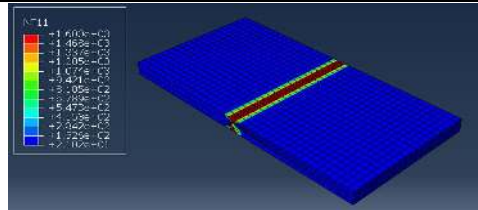| Type of materials welding	Groove Type	Groove geometries	Thermal Analysis	
			Nodal Temperature Distribution	Heat Flux Distribution
Similar materials Welding	Single V Groove	Single V Groove 90^0		
		Single V Groove 60^0		
		Single V Groove 45^0		
		Single V Groove 30^0		
	Double V Groove	Double V Groove 90^0		
		Double V Groove 60^0		
		Double V Groove 45^0		
		Double V Groove 30^0		

Dissimilar materials Welding	Single V Groove	Single V Groove 90^0		
		Single V Groove 60^0		
		Single V Groove 45^0		
		Single V Groove 30^0		
	Double V Groove	Double V Groove 90^0		
		Double V Groove 60^0		
		Double V Groove 45^0		
		Double V Groove 30^0		
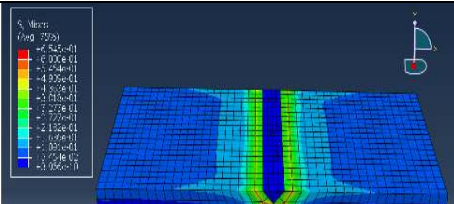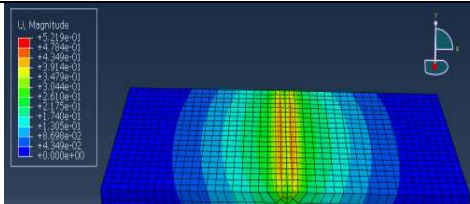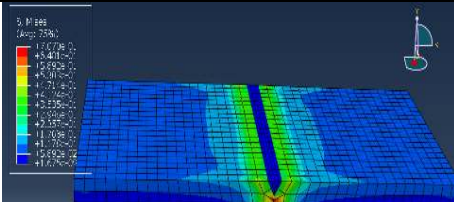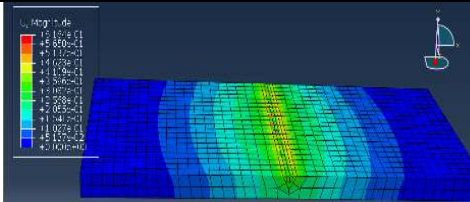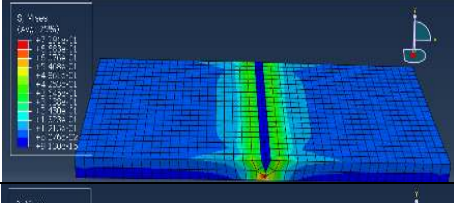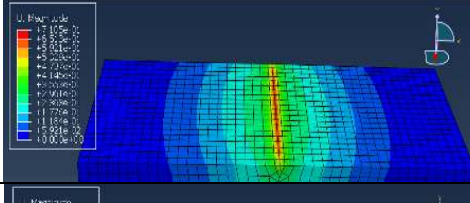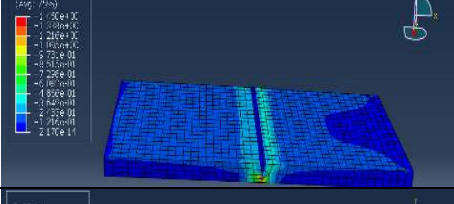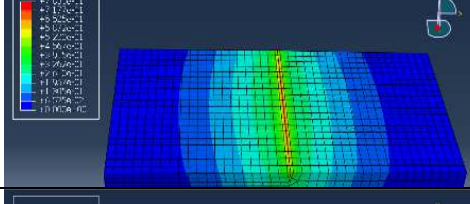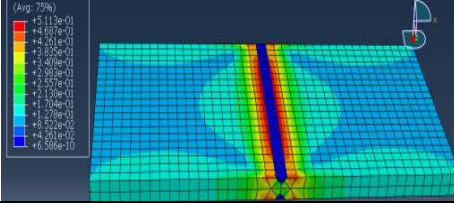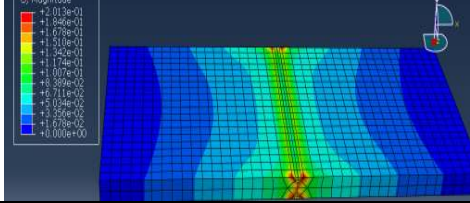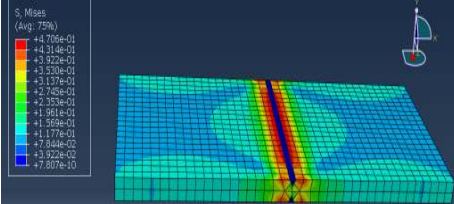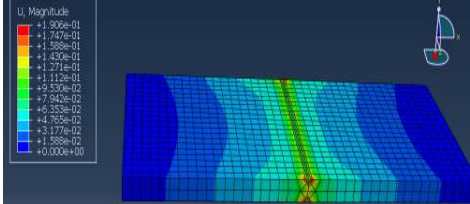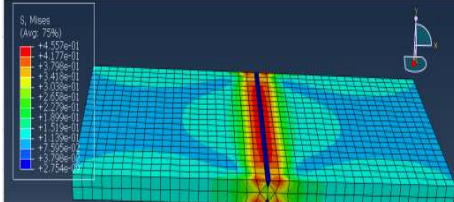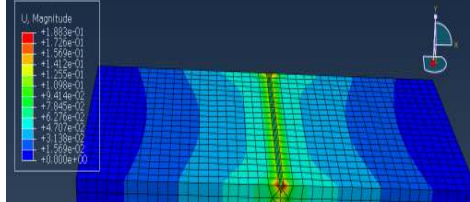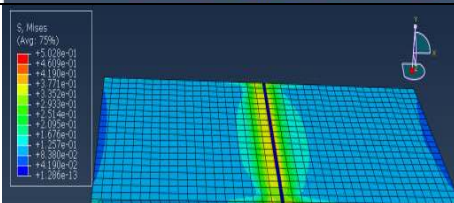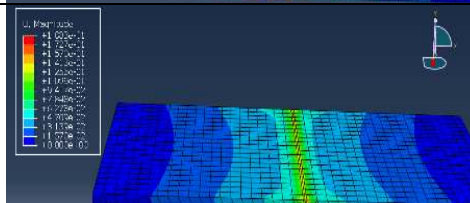
Table 5. Structural analysis results for similar and dissimilar materials welding

Type of materials welding	Groove Type	Groove geometries	Structural Analysis	
			Residual Stresses Distribution	Deformation
Similar materials Welding	Single V Groove	Single V Groove 90^0		
		Single V Groove 60^0		
		Single V Groove 45^0		
		Single V Groove 30^0		
	Double V Groove	Double V Groove 90^0		
		Double V Groove 60^0		
		Double V Groove 45^0		
		Double V Groove 30^0		

		Single V Groove 90[0]		
		Single V Groove 60[0]		
	Single V Groove	Single V Groove 45[0]		
Dissimilar materials Welding		Single V Groove 30[0]		
		Double V Groove 90[0]		
	Double V Groove	Double V Groove 60[0]		
		Double V Groove 45[0]		
		Double V Groove 30[0]		

Table 6. Plotted graphs for similar and dissimilar materials welding

SIMILAR MATERIALS			
Transverse to weld		Longitudinal to weld along thickness	
Single-V Groove	Double-V Groove	Single-V Groove	Double-V Groove
Nodal Temperature Distribution			
Heat Flux Distribution			
Residual stresses Distribution			
Deformation			
DISSIMILAR MATERIALS			
Transverse to weld		Longitudinal to weld along thickness	
Single-V Groove	Double-V Groove	Single-V Groove	Double-V Groove
Nodal Temperature Distribution			

Heat Flux Distribution

Residual stresses Distribution

Deformation

6.2 Thermal analysis of heat flux

In GTAW welding the generated heat flux is utilized to join the metals with succession of melting and solidification. Heat produced at the weld region will produce varying temperatures due to various losses during the weld process. It is stable for initial period and further decreases when power source is switched off. The heat is subsequently lost to surroundings until it equals surrounding conditions. Arc welding uses, arc plasma between two metal electrodes to transfer concentrated energy to the work piece via electrode. This leads to partial melting of the work piece, forming a weld pool. Heat transfer in arc welding is complex, and involve four phases of matter (plasma, gas, liquid, and solid). As mentioned, heat transfer takes place, between the arc and the 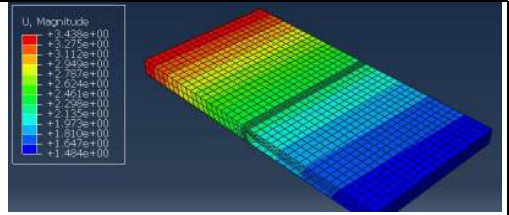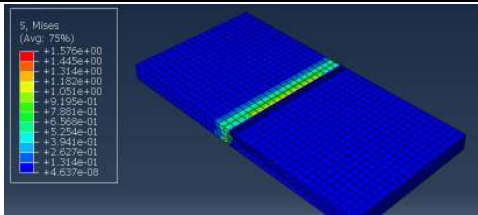electrodes, by droplets of molten metal from the upper electrode, and the solid metal. Under observations of simulation results and plotted graphs, the maximum heat flux was about $3.9 \times 10^4 W/m^2$ in single and double –V 90° grove angle for both similar and dissimilar metal welding. When the volume of molten metal filled is larger, the heat generation is significantly higher, and the minimum heat flux is found to be zero at the non-heat effected zone of the base plate. It is found that large amount of heat flux is observed in V grooves. In welds of dissimilar left side metal plate i.e. mild steel plate absorbs a larger amount of heat flux. The results of heat flux can be seen in Tables 4 and 6.

6.3 Structural analysis of Residual stresses

Residual stresses are the internal stresses generated in material explicit to external forces. After the base plate is welded, the quenching of outer layer weldments by direct contact with water, converts it to martensite but, the inner core of the weldments retains the austenitic form due to insufficient time, for martensitic transformation. The outer layer having martensite structure, is in the state of contraction whereas, the inner core retaining austenite is under expansion. Due to expansion and contraction in a single weldment higher strains are generated, due to which the weld component cannot be used directly in application. The material is tempered to undo the constraints of residual stresses. Comparatively, V-groove have reduced longitudinal stresses over U-grooves. Tensile residual stresses generated in the weld zone are balanced by compressive residual stresses. Surface residual compressive stresses are helpful as, they cancel and reduce the effects produced by applied tensile stresses. Generally, surface compressive stresses are responsible forthe increase of fatigue strength and resistance to stress corrosion cracking. Clamping produces less deformation but more RS, as, it doesn't allow the material to contract or expand freely. Components of high RS deforms during service time. From the above obtained results, the figures justify that high amount of residual stresses (indicated with red colour on plates) are generated in double-V groove as, the volume of the weld bead increases. To avoid this, asuitable V-groove angle is selected to reduce residual stresses. It is

observed that residual stresses generated in double V-grooves are comparatively higher than insingle V-grooves. It is noticed that, large amount of residual stresses is generated in themild steel plate but possess less strength than shipbuilding grade steel. The results of residual stresses can be seen Tables 5 and 6.

6.4 Structural analysis of distortion

Distortion can occur in welding because of non-uniform contraction and expansion of the weldments and base material. The stresses generated during welding cause the base metal to deform. Although, by decreasing the weldment volume, residual stresses can be decreased and distortion can be minimized. The number of passes should be minimized because, with every pass more deformation is produced over a single run. With balancing and positioning the base metal, deformation can be reduced. It can be further reduced by considering the shrinkage allowance before welding and by considering the shortest welding time. Simulations carried are with base metalbeing clamped at both the ends, i.e. arresting all degrees of freedom on the edge sides of the base metal to reduce deformation. From the obtained results, it can be justified that deformation is higher in single V-grooves, compared to double V-grooves. This occurs as the metal surfaces on top and bottom of double V-grooves contract. As, deformations arepresent on both top and bottom surfaces, they cancel each other and balance the overall deformation. Results of deformation can be seen in the Tables 5 and 6.

7. CONCLUSION

The paper produces simulation and numerical analysis of nodal temperature, heat flux, residual stresses, deformation and mechanical properties of low carbon steel (MS) and Ship Building grade during welding, by using multiple software: ABAQUS, MATLAB and R.

1. Simulation on welding of MS plates has been performed under GTAW welding parameters by using ABACUS software.
2. Simulation results are compared with mathematical model, using MATLAB and approximately 12% of error is observed in all of the obtained results.
3. It is observed in simulations, that maximum nodal temperature of the weldment in the fusion zone (1600°C) is similar to the welding torch temperature (1600°C), whereas, heat effected zone varies from 200-1300°C and the rest of the base metal has an ambient temperature of 25°C. More temperature distribution can be observed in larger grooves and hence, the grain structures attained are finer and the produced material is harder.
4. The maximum heat flux is characterized by a single V-groove ($1.3x10^4$W/m^2) weld bead, as the volume of the groove is larger than in the other considered grooves.
5. Maximum percentages of residual stresses are observed in weld beads of Double V-groove as the volume of the molten metal is larger in Double V-groove 90°.

6. It can also be formulated that comparatively less amount of deformation occurs in the double V-groove to the single V-groove.
7. The results are verified for deformation of base plate with and without clamping (fixing at both ends) the plates in the simulation carried out using ABAQUS software. Obtained results show that residual stresses are higher and deformations are lower in weld beads which are clamped.
8. It is not easy to manufacture a component with low residual stresses and low deformation. Hence, to keep low RS, stress relief methods can be used, whereas to keep low distortion, straightening methods are used.
9. Simulations instruct that a large temperature concentration has to be avoided, as large local residual stresses are generated. It does not only result in RS but also results in undesired microstructural changes.
10. As per the results obtained in this work, it can be concluded that residual stresses generated in weld beads can be decreased by maintaining low welding torch temperature, selecting proper dimensions of weld groove (root, land, gap width, thickness of plate, type of groove) and with additive external procedures, i.e. by performing stress relieving procedures.

Hence, with mentioned conclusions it can be stated that these simulations can be exceptionally helpful to diminish the extra loss and provide the ideal environment for GTAW welding.

REFERENCES

[1] Ragotzky, B., Launert, B. and Krausche, T., 2018. Welding simulation for the calculation of the welding residual stresses in welded I-girders. *Kuldeep Virdi and Lauri Tenhunen (Editors)*, p.56.

[2] Fu, D.F., Zhou, C.Q., Can, L.I., Guan, W.A.N.G. and Li, L.X., 2014. Effect of welding sequence on residual stress in thin-walled octagonal pipe–plate structure. *Transactions of Nonferrous Metals Society of China*, *24*(3), pp.657-664.

[3] Piekarska, W., Rek, K., 2017. Numerical analysis and experimental research on deformation of flat made of TIG welded 0H18N9 steel. *Procedia Engineering*, *177*, pp.182-187.

[4] Acevedo, C., Drezet, J.M., Lefebvre, J.P., D'Alvise, L. and Nussbaumer, A., 2012. Residual Stresses in As-Welded Joints: Finite Element Modeling and Neutron Diffraction Stress Measurements. In *Key Engineering Materials* (Vol. 488, pp. 335-338). Trans Tech Publications.

[5] Fitzpatrick, M.E. et al., 2005. Determination of residual stresses by X-ray diffraction.

[6] Anderoglu, O., 2005. *Residual stress measurement using X-ray diffraction* (Doctoral dissertation, Texas A&M University).

[7] Teng, T.L., Chang, P.H. and Tseng, W.C., 2003. Effect of welding sequences on residual stresses. *Computers & structures*, *81*(5), pp.273-286.

[8] Ranjbarnodeh, E., Serajzadeh, S., Kokabi, A.H., Hanke, S. and Fischer, A., 2011. Finite element modeling of the effect of heat input on residual stresses in dissimilar joints. *The International Journal of Advanced Manufacturing Technology*, *55*(5-8), pp.649-656.

[9] Pouranvari, M., Marashi, S.P.H., 2011. Dissimilar spot welds of AISI 304/AISI 1008: metallurgical and mechanical characterization. *steel research international*, *82*(12), pp.1355-1361.

[10] Xia, J., Jin, H., 2017. Numerical study of welding simulation and residual stress on butt welding of dissimilar thickness of austenitic stainless steel. *The International Journal of Advanced Manufacturing Technology*, *91*(1-4), pp.227-235.

[11] Zubairuddin, M., Albert, S.K., Vasudevan, M., Chaudhari, V. and Suri, V.K., 2014. Finite element simulation of weld bead geometry and temperature distribution during GTA welding of modified 9Cr-1Mo steel and experimental validation. *Journal for Manufacturing Science and Production*, *14*(4), pp.195-207.

[12] Javadi, Y., 2015. Investigation of clamping effect on the welding residual stress and deformation of monel plates by using the ultrasonic stress measurement and finite element method. *Journal of Pressure Vessel Technology*, *137*(1), p.011501.

[13] Mousavi, S.A., Miresmaeili, R., 2008. Experimental and numerical analyses of residual stress distributions in TIG welding process for 304L stainless steel. *journal of materials processing technology*, *208*(1-3), pp.383-394.

[14] Ranjbarnodeh, E., Serajzadeh, S., Kokabi, A.H. and Fischer, A., 2011. Effect of welding parameters on residual stresses in dissimilar joint of stainless steel to carbon steel. *Journal of materials science*, *46*(9), pp.3225-3232.

[15] Balram, Y. and Rajyalakshmi, G., 2019. Thermal fields and residual stresses analysis in TIG weldments of SS 316 and Monel 400 by numerical simulation and experimentation. *Materials Research Express*, *6*(8), p.0865e2.

[16] Capriccioli, A. and Frosi, P., 2009. Multipurpose ANSYS FE procedure for welding processes simulation. *Fusion engineering and Design*, *84*(2-6), pp.546-553.

[17] Edwin Raja Dhas, J., Kumanan, S., 2013. Modeling and prediction of HAZ using finite element and neural network modelling. *Advances in Production Engineering & Management*, *8*(1), pp.13-24.

[18] Moarrefzadeh, A., & Branch, M. (2012). FINITE–ELEMENT ANALYSIS FOR OPTIMIZATION OF SUBMERGED ARC WELDING (SAW) PROCESS. In *16th International Research/Expert Conference" Trends in the Development of machinery and Associated Technology* (pp. 10-12).

[19] Anca, A., Cardona, A., Risso, J. and Fachinotti, V.D., 2011. Finite element modeling of welding processes. *Applied Mathematical Modelling*, *35*(2), pp.688-707.

[20] Mahapatra, M.M., Datta, G.L., Pradhan, B., 2006. Three-dimensional finite element analysis to predict the effects of shielded metal arc welding process parameters on temperature distributions and weldment zones in butt and one-sided fillet welds. *Proceedings of the Institution of Mechanical Engineers, Part B: Journal of Engineering Manufacture*, *220*(6), pp.837-845.

[21] Starvin, M.S. et al.: 2018. Numerical simulation of creep behaviour of 316LN stainless steel weld joint. *Materials Today: Proceedings*, *5*(2), pp.8193-8198.

[22] Veljić, D.M., Rakin, M.P., Perović, M.M., Medjo, B.J., Radaković, Z.J., Todorović, P.M. and Pavišić, M.N., 2013. Heat generation during plunge stage in friction stir welding. *Thermal Science*, *17*(2).

[23] Yaghi, A.H., Tanner, D.W.J., Hyde, T.H., Becker, A.A. and Sun, W., 2011, May. Abaqus Thermal Analysis of the Fusion Welding of a P92 Steel Pipe. In *Simulia Customer Conference* (pp. 622-638).

[24] ABAQUS. Analysis user's manual version 6.9 (Dassault Systems, 2009).

[25] Shubert, M. and Pandheeradi, M., 2014. An Abaqus Extension for 3-D Welding Simulations. In *Materials Science Forum* (Vol. 768, pp. 690-696). Trans Tech Publications.

[26] Masubuchi, K., 2013. *Analysis of welded structures: residual stresses, distortion, and their consequences* (Vol. 33). Elsevier.

[27] Goldak, J. et al.: 1984. A new finite element model for welding heat sources. *Metallurgical transactions B*, *15*(2), pp.299-305.

[28] Deng, D. and Murakawa, H., 2008. Prediction of welding distortion and residual stress in a thin plate butt-welded joint. *Computational Materials Science*, *43*(2), pp.353-365.

NOMENCLATURE

S_w	Strength of the weld
F_w	Maximum breaking force at the weld section
A_w	Area of the weld section
S_{BM}	Strength of the base material
F_{BM}	Maximum breaking force at the base material section
A_{BM}	Area of the base material section
t_e	effective throat of weld or the shortest distance between the root of joint to the face of the weld
D	Depth of penetration
L_w	Weld length
K_w	Strength per inch of the weld
P_n	parameterized design load
F_{EX}	Weld stress corresponding to X limits of yield strength of base material
F_y	Shear strength of weld as a function of electrode
A_{nv}	net area subjected to shear which is the effective area of the weld
A_{gt}	gross cross-sectional area of the plate which is subjected to shear loading

a	Diffusivity
Y	desired effect
X	spatial resolution
b_0	Base material properties
i	Beads along the axial direction of the weldment
j	Nodes along the transverse direction of the weldment
b_i	Weldment properties as a function of Base material properties and groove dimensions
b_{ij}	Nodal resolution of the weldment properties
x_i	Unit vector along the axial direction of the weldment
y_j	Unit vector along the transverse direction of the weldment
Y	nodal factor
n	Total number of nodes
T	Temperature at any time instant
T_0	initial temperature or room temperature (27^0 C)
v	welding speed
k	Thermal conductivity
R	Resistance of the electrode
V	Voltage
I	Current
Q	heat utilised
t	time

Greek symbols

α	Groove angle
ϕ	Correction factor (0.75)
λ	Thermal diffusivity

СТРУКТУРНА И ТЕРМИЧКА АНАЛИЗА ЧЕОНОГ СПОЈА ЗАВАРЕНОГ GTAW ПОСТУПКОМ КОРИШЋЕЊЕМ СЛИЧНИХ И РАЗЛИЧИТИХ МАТЕРИЈАЛА ПРИ ОДРЕ- ЂЕНИМ УГЛОВИМА ЖЛЕБА ПРИМЕНОМ СИМУЛАЦИЈЕ И МАТЕМАТИЧКОГ МОДЕЛИРАЊА

Б. Киран, К. Мишра, Р.Ј. Синг, Д. Нагараџу

Рад се бави симулацијом и математичким модели- рањем различитих параметара који се користе при наношењу једноструких и двоструких варова код чеоног споја са V жлебом. Изабрани материјали су били челик EN 10025 (класа S259) и бродограђевни челик D36 због њихове широке употребе у индустрији и отпорности на корозију. Симулација је извршена при угловима жлеба од 90^0, 60^0, 45^0 и 30^0 са сличним и различитим базним металима у циљу предвиђања деформације, дистрибуције резидуалног напона, топлотног флукса и нодалне температуре коришћењем софтверског пакета ABAQUS. Матема- тички модел је развијен помоћу алата MATLAB за даље предвиђање дистрибуције температуре и укупне концентрације напона у свакој локализованој нодалној тачки. Модел се може користити за добијање оптималних параметара заваривања као што су вар, брзина којом лет лампа постиже темпе- ратуру, напон и добија напајање. На основу резул- тата изведен је јасан закључак: симулација је показала да је угао од 45^0 најефикаснији при нано- шењу једноструког и двоструког вара код чеоног споја са V жлебом.